JOURNAL OF VIROLOGY, Feb. 2000, p. 1948–1960 Vol. 74, No. 4
0022-538X/00/$04.00+0

Selective Interactions of Polyanions with Basic Surfaces on Human Immunodeficiency Virus Type 1 gp120

MAXIME MOULARD,[1]† HUGUES LORTAT-JACOB,[2] ISABELLE MONDOR,[1] GUILLAUME ROCA,[1] RICHARD WYATT,[3] JOSEPH SODROSKI,[3] LU ZHAO,[4] WILLIAM OLSON,[4] PETER D. KWONG,[5] AND QUENTIN J. SATTENTAU[1]*

Centre d'Immunologie de Marseille-Luminy, 13288 Marseille Cedex 9,[1] and Institut de Biologie Structurale, 38027 Grenoble Cedex 01,[2] France; Department of Cancer Immunology and AIDS, Dana-Farber Cancer Institute, Harvard Medical School, Boston, Massachusetts 02115[3]; Progenics Pharmaceuticals Inc., Tarrytown, New York 10591[4]; and Department of Biochemistry and Molecular Biophysics, College of Physicians and Surgeons, Columbia University, New York, New York 10032[5]

Received 25 June 1999/Accepted 17 November 1999

It is well established that the gp120 V3 loop of T-cell-line-adapted human immunodeficiency virus type 1 (HIV-1) binds both cell-associated and soluble polyanions. Virus infectivity is increased by interactions between HIV-1 and heparan sulfate proteoglycans on some cell types, and soluble polyanions such as heparin and dextran sulfate neutralize HIV-1 in vitro. However, the analysis of gp120-polyanion interactions has been limited to T-cell-line-adapted, CXCR4-using virus and virus-derived gp120, and the polyanion binding ability of gp120 regions other than the V3 loop has not been addressed. Here we demonstrate by monoclonal-antibody inhibition, labeled heparin binding, and surface plasmon resonance studies that a second site, most probably corresponding to the newly defined, highly conserved coreceptor binding region on gp120, forms part of the polyanion binding surface. Consistent with the binding of polyanions to the coreceptor binding surface, dextran sulfate interfered with the gp120-CXCR4 association while having no detectable effect on the gp120-CD4 interaction. The interaction between polyanions and X4 or R5X4 gp120 was readily detectable, whereas weak or undetectable binding was observed with R5 gp120. Analysis of mutated forms of X4 gp120 demonstrated that the V3 loop is the major determinant for polyanion binding whereas other regions, including the V1/V2 loop structure and the NH_2 and COOH termini, exert a more subtle influence. A molecular model of the electrostatic potential of the conserved coreceptor binding region confirmed that it is basic but that the overall charge on this surface is dominated by the V3 loop. These results demonstrate a selective interaction of gp120 with polyanions and suggest that the conserved coreceptor binding surface may present a novel and conserved target for therapeutic intervention.

A number of pathogenic microorganisms attach to cell surfaces via heparan sulfate proteoglycans (HSPG). Of these, several viruses appear to use HSPG at a step prior to interaction with their specific receptors. Thus, herpes simplex virus (81), pseudorabies virus (27), human herpesvirus 7 (71), adeno-associated virus (76), dengue virus (10), and vaccinia virus (13) can all interact with cell surface HSPG. The crystal structure of a complex formed by foot-and-mouth disease virus and heparin has recently been determined (29). Human immunodeficiency virus type 1 (HIV-1) binds cell surface HSPG, and the type and quantity of HSPG on a given cell type modulate virus infectivity in vitro (50, 57, 59, 65) and may influence viral tropism in vivo (83).

It is well established that HIV-1 can interact with soluble polyanions and cell surface HSPG via the gp120 V3 loop; polyanions such as dextran sulfate (DexS) compete with V3 loop-specific monoclonal antibodies (MAbs) for binding (3, 8, 32, 63, 65) but interfere weakly or undetectably with soluble-gp120–CD4 binding (8, 33). Moreover, radioactively labeled heparin binds V3 loop peptides and recombinant gp120 (3, 33), and various polyanions neutralize the infectivity of T-cell-line-adapted (TCLA) HIV-1 at low (micromolar) concentrations (2, 41, 48, 82). The V3 loop-HSPG association is thought to take place via electrostatic interactions between the acidic sulfate groups on heparan sulfate and basic residues within the V3 loop. Indeed, some TCLA viruses, such as the HXBc2 molecular clone, have a V3 loop with a net charge of +9 and a sequence motif of X-B-B-B-X-B-X-X-B-X (where X is a hydropathic residue and B is a basic residue), similar to the motifs described for other heparin-protein interactions (27). However, not all strains of HIV-1 have such basic V3 loops; those of CCR5-using (R5 [4]) viruses are substantially less basic than those of CXCR4-using (X4 [4]) and dualtropic, CCR5- and CXCR4-using (R5X4 [4]) viruses (28, 42), and primary isolate (PI) X4 viruses tend to have less-basic V3 loops than TCLA X4 viruses. The level of positive charge present on the gp120 surface may relate directly to coreceptor utilization, in that the exposed surface of CXCR4 has been modeled as highly acidic whereas that of CCR5 appears to be less so (17, 42). However, a recent study suggests that negatively charged moities, including acidic amino acids and sulfated tyrosine residues, may be important for binding of gp120 to both CCR5 and CXCR4 (24).

The solution of the crystal structure of the gp120 core complexed with domains 1 and 2 of CD4 and an Fab fragment of a neutralizing MAb (44) has generated a great deal of information with respect to gp120-CD4 interactions (44, 90), gp120-coreceptor interactions (44, 64), and gp120-antibody interac-

* Corresponding author. Present address: Imperial College of Science, Technology and Medicine, Jefferiss Research Trust Laboratories, Norfolk Pl., London W2 1PG, England. Phone: 44-171 886 1539. Fax: 44-171 886 6645. E-mail: quentin.sattentau@pathology.oxford.ac.uk.

† Present address: Department of Immunology, The Scripps Research Institute, La Jolla, CA 92037.

tions (88). Within this structure, the Fab fragment (17b) binds an epitope that comprises part of the CD4-induced (CD4i) region, so called because it becomes more accessible after CD4 binding (75, 77, 89). A comprehensive mutagenesis study based on the R5 $gp120_{YU2}$ has defined this region as a coreceptor binding surface that is highly conserved among HIV-1, HIV-2, and simian immunodeficiency virus isolates (64). It seems likely, based on experimental and structural evidence, that this surface is at least partially masked by the V1/V2 and V3 loops in the intact gp120-gp41 trimer, and CD4 binding displaces these variable loops, revealing the conserved surface (44, 64, 68, 75). The coreceptor binding site on gp120 most likely consists of both the V3 loop, which defines coreceptor specificity (12, 14, 37, 38), and the conserved surface, which mediates tight attachment to the coreceptor and the induction of conformational changes within the gp120 oligomer (38, 44, 64, 68). One striking aspect of the conserved coreceptor binding domain is its basic nature; seven basic amino acids are located within a relatively restricted surface on $gp120_{YU2}$ (64). We speculated that as a result of its positive charge and high degree of conservation, this surface might bind polyanions and be a potential target for attack by such molecules. Here we provide evidence, obtained by MAb inhibition studies and labeled-heparin binding and surface plasmon resonance (SPR) analyses, that the conserved coreceptor binding surface in association with the V3 loop on X4 and R5X4 gp120, but not R5 gp120, binds polyanions. Based on these data and a molecular model of the electrostatic potential on this surface of gp120, we propose that HSPG binding probably takes place initially via a selective and high-affinity interaction with the gp120 V3 loop followed by a second, lower-affinity interaction with the conserved coreceptor binding surface. These interactions may have implications for HIV tropism and replication in vitro and in vivo and may allow for the development of inhibitors with therapeutic potential.

MATERIALS AND METHODS

Antisera, MAbs, and recombinant proteins. The anti-CD4 mouse MAb Q4120 (from H. Holmes and the MRC AIDS Reagent Project, Potters Bar, United Kingdom), which was previously mapped to the first domain of CD4, competes with gp120 for CD4 binding (35). Pooled HIV immune immunoglobulin (61) was obtained from the AIDS Reagent Repository, National Institutes of Health (NIH), Bethesda, Md. The following HIV-1 gp120-specific MAbs of human origin were used (their specificities are in parentheses): 21h (CD4 binding site [CD4bs]), 19b (V3 loop) (53), 17b, and 48d (CD4i epitope) (77) were from J. Robinson (University of Connecticut), and 447-52D (V3 loop) (15, 31) was purchased from Cellular Products Inc., Buffalo, N.Y. The chimpanzee anti-gp120-V2 MAb C108G, prepared as previously described (86), was obtained from S. Tilley, Public Health Research Institute, New York, N.Y. The anti-CD4bs (IgG1b12) (7) and anti-V3 loop (Loop 2) (18) monospecific antibodies were from D. Burton, Scripps Research Institute, La Jolla, Calif. The human anti-gp120 MAb 2G12 (79, 80) was from A. Trkola, Aaron Diamond AIDS Research Center, New York, N.Y. Murine MAb G3-136 (V2 specific) was from Tannox Biosystems Inc., Houston, Tex. and D. D. Ho (Aaron Diamond AIDS Research Center), SC258 was from Abbott Laboratories, 9284 (V3 specific) was from NEN Life Science Products (Le Blanc Mesnil, France), and 110.I (V3 specific) was from F. Traincard, Institut Pasteur, Paris, France. The D7324 antibody, specific for a conserved region of the gp120 COOH terminus, was obtained from Aalto Bioreagents, Dublin, Ireland. Recombinant soluble CD4 (sCD4) prepared in Chinese hamster ovary (CHO) cells was prepared by R. Sweet, SmithKline and Beecham (King of Prussia, Pa.) (16) and was obtained from the NIH AIDS Reagent Repository. Recombinant soluble gp120 (sgp120) IIIB (BH10), HxBc2, and MN were derived from X4 TCLA viruses, SF-2 is from an R5X4 TCLA virus, 89.6 and W61D are from R5X4 PI viruses, and Bal and JRFL are from R5 PI viruses (19). IIIB, MN, W61D, and SF2 were obtained from the MRC AIDS Reagent Project, and Bal was from R. Sweet, SmithKline and Beecham. The V3-deleted form of JRFL was prepared as previously described (78). Wild-type (WT) $gp120_{HXBc2}$ was derived from the IIIB X4 TCLA isolate of HIV-1, and mutants in which the COOH and NH_2 termini and the V1/V2 and V3 loops were deleted were prepared as previously described (89, 91). sgp120 was prepared either from purified CHO cell supernatants (IIIB, SF-2, JRFL, and JRFLΔV3) or from *Drosophila* cells (MN, Bal, 89.6, HXBc2, and mutants thereof).

Polyanion inhibition of MAb binding to monomeric gp120 detected by ELISA. DexS, dextran, chondroitin sulfate, heparin, pentosan sulfate (PS), and aurintricarboxylic acid (ATA) were obtained from Sigma-Aldrich (Saint Quentin Fallavier, France). The interaction between monomeric recombinant sgp120 and polyanions was measured by a sandwich enzyme-linked immunosorbent assay (ELISA). Ninety-six-well Maxisorp ELISA plates (Nunc; Polylabo, Strasbourg-Meinau, France) were coated overnight at 4°C with 50 μl of a 5-μg/ml solution of D7324 in carbonate buffer (pH 8.5). Plates were washed twice in 25 mM Tris-HCl (pH 8.0)–150 mM NaCl–0.05% Tween 20 (ELISA buffer [EB]), then saturated with 2% bovine serum albumin (BSA) in phosphate-buffered saline (PBS) for 1 h at room temperature (RT). After two washes with EB, sgp120 was captured for 3 h at RT. Plates were washed six times and then incubated with 50 μl of one of the polyanions, at various concentrations, in PBS–2% BSA for 30 min at RT. Either MAbs were added directly to the mixture or, in some experiments, the plates were washed twice before MAb addition. After incubation of plates for 1 h at RT followed by six washes, bound MAbs were detected with either peroxidase-conjugated goat anti-mouse immunoglobulin G (IgG) (1/2,500; Immunotech, Marseille, France) or peroxidase-conjugated goat anti-human IgG (1/5,000) in PBS–2% BSA by incubation for 1 h at RT. Detection was carried out with a Sigma Fast *o*-phenylenediamine dihydrochloride kit from Sigma-Aldrich in accordance with the supplier's recommendations. For detection of polyanion inhibition of MAb binding to gp120 complexed with sCD4, two methods were used. In the first assay format, gp120 captured onto ELISA plates as described above was incubated with a 1-μg/ml solution of sCD4 for 1 h at RT, and then the plates were washed before MAbs were added as in the original assay. In the second assay format, ELISA plates were coated with the anti-CD4 MAb L120 overnight at 4°C, then blocked with PBS–2% BSA for 1 h at RT. After two washes of the plates with EB, sCD4 was added at 1 μg/ml and the plates were incubated for 3 h at RT. The plates were washed six times in EB, then incubated with sgp120 at 1 μg/ml for 3 h at RT. Following six washes of the plates with EB, polyanion diluted in PBS–2% BSA was added at various concentrations and the plates were incubated for 30 min at RT. MAbs were added, and the plates were incubated for 1 h at RT before detection of binding as described above.

Polyanion inhibition of MAb binding to HIV-1-infected cells. The T-cell line H9, obtained from M. Popovic and R. Gallo and supplied by the MRC AIDS Reagent Project, was grown in RPMI 1640 supplemented with 10% fetal calf serum (FCS), H9 cells were infected with either the HIV-1 TCLA X4 molecular clone HX10 (obtained from B. Hahn, University of Alabama—Birmingham and A. Fisher, Royal Post Graduate Medical School, Hammersmith Hospital, London, United Kingdom) (25) or the HIV-1 TCLA X4 MN isolate (obtained from R. Gallo via the NIH AIDS Repository) for 8 to 10 days. At this time postinfection there was no detectable CD4 remaining at the cell surface or syncytium formation in the culture, but strong Env expression was detected using gp120-specific MAbs and flow cytometry (see below). The interaction of the polyanions with the infected cells was detected indirectly by measuring inhibition of MAb binding to cell surface Env. Infected H9 cells (4×10^5) were washed with PBS–1% FCS–0.02% sodium azide (wash buffer [WB]) and resuspended in 50 μl of WB containing polyanions at the appropriate concentration. After a 2-h incubation at 37°C, the cells were washed twice in WB and then incubated with MAbs. After a 1-h incubation with agitation at 4°C, the cells were washed twice in WB and fixed overnight with 0.5% formaldehyde at 4°C. The cells were washed twice, and then a goat anti-human IgG–phycoerythrin conjugate (Immunotech) was added at a 1/100 dilution in WB. After a further 1-h incubation at 4°C with agitation, the cells were washed twice, resuspended in 200 μl of WB, and analyzed by single-color flow cytometry with a FACScan (Becton Dickinson, San Diego, Calif.) equipped with Lysis II software. Each datum point represents the acquisition of 10,000 events gated on side and forward light scatter and is the mean of data from triplicate samples.

DexS inhibition of gp120-CXCR4 interactions. The assay used to measure DexS inhibition of gp120-CXCR4 interactions was a modified version of a previously described method (50, 84). Briefly, sgp120 at 30 μg/ml that had or had not been preincubated with various concentrations of DexS for 30 min at RT was incubated with 10^6 A3.01 cells (obtained from T. Folks, Centers for Disease Control and Prevention, Atlanta, Ga.) in a total volume of 50 μl for 1 h at 37°C with agitation. Each sample was divided into five aliquots, one of which was incubated directly with Q4120 (2 μg/ml) and three (replicates) of which were incubated with 12G5 (5 μg/ml) in a total volume of 50 μl for 1 h at 4°C with agitation. The fifth aliquot was washed twice in WB and incubated with either HIV immune immunoglobulin (100 μg/ml) or MAb 2G12 (10 μg/ml) for direct detection of gp120 bound at the cell surface. The cells were subsequently washed in WB, and bound MAb was labeled with phycoerythrin-conjugated goat anti-mouse IgG (Immunotech) at a 1/200 dilution or a goat anti-human IgG–phycoerythrin conjugate (Immunotech) at a 1/100 dilution for 1 h at 4°C with agitation. After the cells were washed in WB, bound antibody was detected by flow cytometric analysis as described above. Percent inhibition of Q4120 and 12G5 binding was calculated by using the equation $100 - [(t - c)/(m - c) \times 100]$, where t represents the signal for the test sample, c represents background staining in the absence of MAb, and m represents staining in the absence of inhibitor (gp120). Percent reduction of inhibition of 12G5 binding was calculated by taking the maximum inhibition of 12G5 binding in the presence of sgp120 as 0% and no

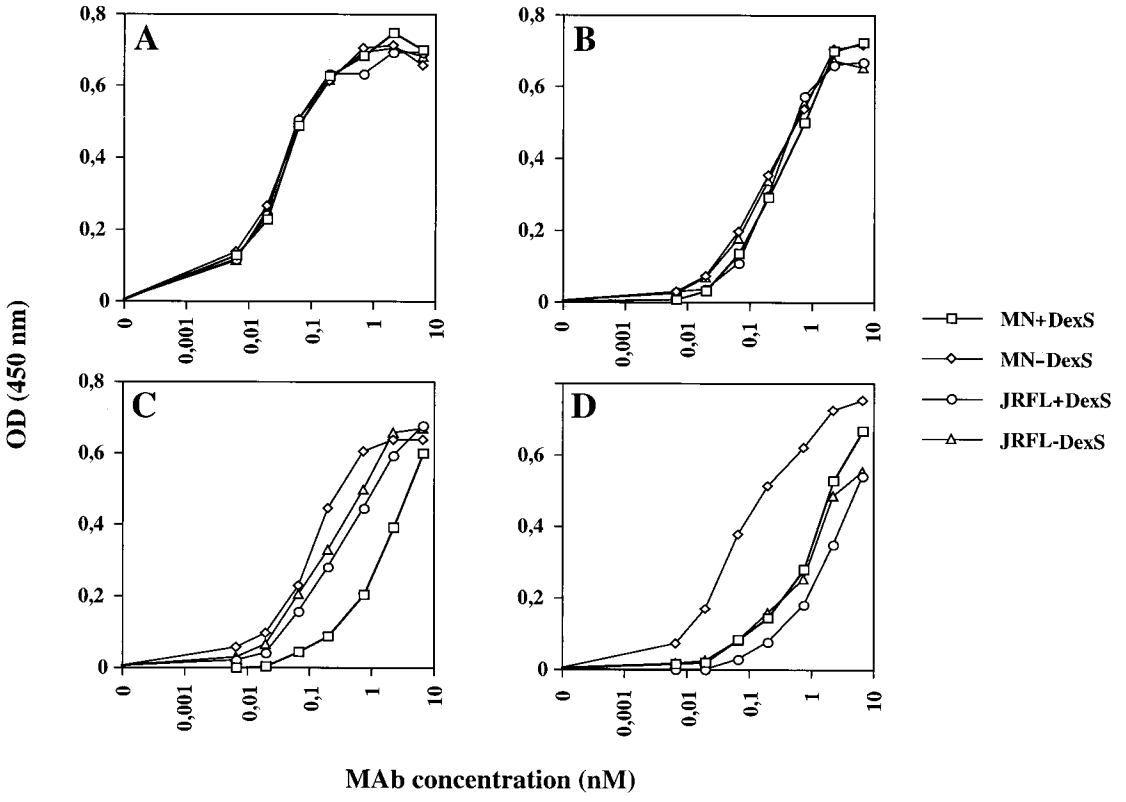

FIG. 1. DexS inhibition of MAb binding to the conserved coreceptor binding site. Monomeric recombinant sgp120 derived from the MN or JRFL strain of HIV-1 was captured on the solid phase by an antibody to the conserved COOH terminus, then preincubated without (−) or with (+) 12.3 μM DexS prior to addition of sequential dilutions of gp120 antibodies specific for the CD4bs (IgG1b12) (A), the V3 loop (447-52D) (B), and the CD4i epitopes 17b (C) and 48d (D). Detection of bound MAb was carried out by ELISA, and the results are presented as optical densities at 450 nm. Each datum point is the mean of values obtained from triplicate samples, and each experiment was repeated on at least three separate occasions.

inhibition of 12G5 binding in the absence of sgp120 as 100%. The absence of a direct effect of DexS on the binding of MAbs Q4120 and 12G5 was determined without sgp120, and, similarly, no effect of DexS on 2G12 binding to gp120 was observed.

DexS inhibition of HIV-1 infectivity. HIV-1 clones HXBc2 (TCLA X4) and JRCSF (PI R5) were obtained from J. Moore, Aaron Diamond AIDS Research Center, and the NIH AIDS Research and Reference Reagents Program, Bethesda, Md., respectively. Infectious stocks of these viruses were prepared by infecting peripheral blood lymphocytes (PBL) previously activated for 3 days with phytohemagglutinin at 1 μg/ml and cultured in RPMI 1640 supplemented with 10% heat-inactivated FCS and 40 IU of interleukin-2 (growth medium [GM]). Approximately 100 50% tissue culture infective doses of each virus was preincubated with various concentrations of DexS, in a total volume of 100 μl, for 1 h at 37°C in a U-bottomed 96-well plate (Nunc). PBL at 5×10^4/well in 100 μl of GM were added to the virus-DexS mixture, which was then incubated for a further 2 h at 37°C with agitation. The cells were washed and resuspended in GM at 200 μl/well. After 7 days of culture, during which the cells were maintained at 1×10^6 to 2×10^6/ml, 100 μl of supernatant was harvested from each well and tested for cell-free p24 activity as previously described (51). Results are expressed as medians of data for three replicate wells ± 1 standard deviation. Chondroitin sulfate and dextran, used as negative controls, consistently failed to reduce infectivity of either virus at the same concentrations as those at which DexS was used (results not shown).

Binding of [^{35}S]heparin to gp120. To measure binding of ^{35}S-labeled heparin to gp120, we used a technique adapted from one described in reference 33. Briefly, ^{35}S-labeled heparin (40 μg/ml, corresponding to approximately 6 μCi) (Amersham Ltd., Little Chalfont, United Kingdom) was incubated overnight at RT with WT sgp120, mutated forms thereof, or sgp120 precomplexed for 1 h at RT with a fivefold molar excess of MAb in 25 mM Tris-HCl buffer, pH 7.5, at various concentrations in total volumes of 90 μl. Three 30-μl aliquots of each incubation mixture were filtered through a reinforced nitrocellulose membrane filter (0.2-μm pore size; Cellulosensitrat BA 83; Schleicher and Schuell, Dassel, Germany) by using a 96-well micromanifold (Anderman and Co., Kingston, United Kingdom). The wells were washed twice in Tris-HCl buffer, and the filtered areas were excised and individually placed in scintillation vials containing 200 μl of 2 M NaCl. The vials were shaken for 1 h before addition of 4 ml of scintillation fluid (Ecoscint; Packard, Meriden, Conn.). ^{35}S radioactivity was then measured on a Beckman LS 6500 scintillation counter. In some experiments, the specificity of the interaction was determined by preincubation of the sgp120 with an excess of unlabeled heparin prior to addition of the [^{35}S]heparin. Negative controls measured [^{35}S]heparin binding to the filter in the absence of any protein or in the presence of MAbs such as 48d; similar levels of binding were obtained in both cases.

Kinetic analysis of gp120-heparin interactions by SPR. Size-fractionated, biotinylated heparin was immobilized onto a streptavidin-coated Biacore B1 sensor chip at densities yielding 65, 35 or 20 resonance units (RU) to determine the optimal concentration for sgp120 binding. WT or mutant sgp120 in Tris-buffered saline was reacted with the sensor chip at flow rates of 5 to 15 μl/min. These initial studies demonstrated that a maximum density of 20 to 25 RU of heparin was required to give a detectable signal but avoid the mass transport effect, and these densities were used for all subsequent kinetic studies. In a typical analysis, several concentrations of gp120 (see legend to Fig. 6) were injected onto the heparin-coated surface at a flow rate of 15 μl/min for 6 min, after which the complexes were rinsed with buffer to analyze the dissociation phase. In other studies, the association phase was allowed to proceed to equilibrium, which took 20 min. Subsequently, the heparin surface was regenerated with a 6-min pulse of Tris-buffered saline containing 1.0 M NaCl. Sets of sensorgrams were analyzed by global fitting of the data, using BIAevaluation 3.0 software.

Electrostatic modeling of the gp120 trimer. To analyze the influence of V3 loop charge on the overall electrostatic potential of the conserved coreceptor binding surface, we carried out modeling, as described in reference 45, based on the HXBc2 crystal structure of the monomeric gp120 core (44), in which optimization of quantifiable surface parameters was used to model precisely the gp120 core structure. Variations in the structure of the V3 loop were found to have little influence on the contribution of the V3 electrostatic component to the overall electrostatic potential (45). The models used here comprise a composite model of the MN V3 loop nuclear magnetic resonance structure (9) grafted onto the HXBc2 gp120 core X-ray structure (44). For the gp120s derived from the HXBc2, 89.6, MN, and JRFL isolates, homology modeling was carried out by using the program PrISM (A.-S. Yang and B. Honig, Columbia University, unpublished data), thus adapting the initial composite model to the correct sequence for each gp120. Because of the large sizes of the trimeric models, the

TABLE 1. DexS inhibition of MAb binding to gp120

Epitope	MAb	Fold reduction in half-maximal MAb binding to gp120 of[a]:	
		IIIB (X4)	JRFL (R5)
V2	G3-136	1.0	NB[b]
	SC258	1.0	1.0
	C108G	8.6	NB
V3	9284	5.0	NB
	110.I	100	NB
	50-23	1.2	NB
	Loop2	NB	3.0
	19b	NB	1.4
	447-52D	NB	1.1
CD4bs	IgG1b12	1.9	1.5
	21h	1.0	1.0
CD4i	17b	50.0	1.8
	48d	37.0	2.4
Other	2G12	1.0	1.5

[a] Inhibition studies were performed in the presence of 12.3 μM DexS.
[b] NB, no significant MAb binding to gp120 species.

electrostatic potentials were calculated with the program Delphi (55), using a 129-division grid, which corresponds to 1.2 Å per grid segment. Although small local deviations can be observed as a result of the grid approximation used in the calculation of the potential, the overall calculation is highly accurate (39).

RESULTS

Polyanions selectively inhibit binding of MAbs to the gp120 V3 loop and the CD4i epitopes. Previous studies have demonstrated that polyanions inhibit binding of MAbs to the V3 loop of TCLA X4 gp120. To investigate whether polyanions are also able to interact with other regions of gp120, we tested the ability of DexS, a well-characterized polyanion with relatively potent gp120 V3 loop binding activity, to interfere with the binding of a panel of gp120-specific MAbs in an ELISA. We initially chose to study gp120 derived from the following viruses: MN, an X4 TCLA HIV-1 isolate, and JRFL, an R5 clone. Four MAbs that are known to react with both gp120s were selected: 447-52D (specific for V3), IgG1b12 (specific for the CD4bs), and 17b and 48d (specific for CD4i). As shown in Fig. 1, DexS at 12.3 μM, a dose previously demonstrated to inhibit substantially TCLA HIV-1 infectivity (see Fig. 4), reduced the binding of MAbs 17b and 48d to $gp120_{MN}$ by approximately 10- and 30-fold, respectively, as determined by measuring the displacement of the antibody binding curves, but had only a very weak effect on their binding to $gp120_{JRFL}$. The binding of MAbs IgG1b12 and 447-52D to both gp120s was unaffected by DexS, confirming data of a previous study (65) demonstrating that the CD4bs and certain V3 loop epitopes are unaffected or only weakly affected by polyanions. To further dissect the effect of polyanions on MAb binding to gp120, we tested the ability of DexS to interfere with the binding of a number of MAbs to different epitopes on $gp120_{IIIB}$ (TCLA X4) and $gp120_{JRFL}$. These MAbs were chosen because they bind neutralizing epitopes on monomeric gp120 that are well exposed on the virion-associated trimeric form of gp120 (52, 69). As shown in Table 1, substantial reductions in half-maximal (50%) MAb binding to IIIB gp120 were seen for the V3 loop MAbs 9284 and 110.I (5- and 100-fold reductions, respectively) and the two CD4i MAbs 17b and 48d (50- and 37-fold, respectively). Moderate (8.6-fold) inhibition was observed for the V2-specific MAb C108G, whereas inhibition of MAbs specific for the CD4bs and the 2G12 epitopes was weak or absent. By contrast, little inhibition of binding of any MAb was observed for JRFL: only the V3 loop-specific MAb Loop 2 and the CD4i-specific MAbs 17b and 48b demonstrated reductions in 50% binding (3.0, 1.8, and 2.4-fold, respectively). We evaluated the ability of DexS to interfere with binding of 17b and 48d to gp120 molecules with different viral origins and coreceptor usages: gp120 BH10; MN (TCLA X4), SF2 (TCLA R5X4), 89.6, and W61D (PI R5X4); and JRFL and Bal (PI R5). DexS potently inhibited binding of 48d and 17b to gp120 BH10 (IIIB), MN, SF-2, 89.6, and W61D but had little or no effect on IgG1b12 binding (Table 2). By contrast, DexS had more subtle effects on MAb binding to the R5 gp120 molecules. Inhibition of 48d and 17b binding to JRFL was very weak (maximum, 2.4-fold), whereas inhibition of binding of the same MAbs to Bal gp120 was intermediate (5- to 6-fold). Finally, we tested the abilities of other polyanions to interfere with the binding of 17b and 48d to gp120. ATA, PS, and heparin are all anionic and have been previously demonstrated to reduce HIV infectivity, whereas dextran (uncharged) and chondroitin sulfate (weakly anionic) do not. The spectrum of potency observed for inhibition of 17b binding by the different polyanions was ATA > DexS > PS, with dextran and chondroitin sulfate failing to interfere with the binding of any MAb (results not shown).

Influence of sCD4 binding on DexS inhibition of CD4i-specific MAbs. To investigate whether the inability of polyanions to interfere with binding of 17b and 48d to $gp120_{JRFL}$ was a result of masking by the variable loops or an inappropriate conformation of the conserved coreceptor binding region in the absence of CD4, we attempted to inhibit the binding of these MAbs after sCD4 was complexed with gp120. The $gp120_{MN}$-sCD4 complex bound 17b, 48d, and a third CD4i-specific MAb, CG10, with higher affinity than did MN gp120 alone, confirming the CD4-induced nature of these epitopes (Table 3). By contrast, no significant alteration of the V3 loop-specific MAb 447-52D was observed, in accordance with the constitutively well-exposed nature of this epitope. The addition of DexS at 12.3 μM reduced 48d binding similarly regardless of whether sCD4 was complexed (without sCD4 there was a 50-fold reduction, and with sCD4 there was a 43-fold reduction), whereas 17b binding was inhibited by approximately 4-fold more in the presence of sCD4 (without sCD4 there was a 20-fold reduction, while with sCD4 there was an 80-fold reduction). Thus, sCD4 appears to selectively increase the accessibility of the polyanion binding site on MN gp120. Since CG10

TABLE 2. DexS inhibition of MAb binding to gp120 molecules of different origins

MAb	Fold reduction in half-maximal binding of MAb to gp120 of[a]:						
	IIIB (X4)	MN (X4)	SF-2 (X4)	89.6 (R5X4)	W61D (R5X4)	JRFL (R5)	Bal (R5)
IgG1b12	1.9	1.2	1.0	1.3	3.4	1.5	1.2
48d	37.0	40.0	30.0	66.7	5.1	2.4	5.0
17b	50.0	17.7	13.5	7.5	16.5	1.8	6.0

[a] Inhibition studies were performed in the presence of 12.3 μM DexS.

TABLE 3. Effect of sCD4 treatment on DexS inhibition of MAb binding

MAb	DexS treatment[a]	Concn of MAb (nM) required for half-maximal antibody binding[b]			
		MN		JRFL	
		−sCD4	+sCD4	−sCD4	+sCD4
447-52D	No	0.01	0.01	0.01	0.02
	Yes	0.01	0.02	0.02	0.02
CG10	No	NB[c]	0.03	NB	0.13
	Yes	NB	1.99	NB	0.13
17b	No	0.33	0.06	1.91	0.19
	Yes	6.67	4.66	1.91	0.19
48d	No	0.13	0.05	6.66	0.13
	Yes	6.66	1.99	6.66	0.06

[a] sgp120, complexed or not complexed with sCD4, was or was not treated with DexS at 12.3 μM.

[b] sgp120 was (+) or was not (−) pretreated with a molar excess of sCD4 before addition of DexS and/or MAb.

[c] NB, no significant binding to gp120 in the absence of sCD4.

is unable to react with gp120 in the absence of CD4, we were unable to determine polyanion inhibition of this MAb under these conditions. However, the potent inhibition of CG10 binding to the CD4-gp120 complex is consistent with the data obtained for 17b and 48d. The binding of CD4i-specific MAbs to $gp120_{JRFL}$ was increased from approximately 10-fold (17b) to >100-fold (CG10) in the presence of sCD4. However, the increased binding of the CD4i-specific MAbs had little impact on the ability of DexS to interfere with MAb binding to $gp120_{JRFL}$; no significant inhibition of binding of any of the CD4i-specific MAbs was observed under any conditions. The inability of sCD4 complexing to facilitate the binding of DexS to the conserved coreceptor binding site on $gp120_{JRFL}$ implies that the lack of association is constitutive rather than conformational or cryptic.

Polyanions inhibit the binding of MAbs 17b and 48d to oligomeric, functional X4 gp120. Soluble, monomeric gp120 is a useful tool for analyzing a variety of interactions but does not fully represent the behavior of the oligomeric, functional form of the glycoprotein. We therefore attempted to establish whether the binding of polyanions to oligomeric, mature X4 gp120 interfered with the binding of MAbs to the CD4i epitope. For this we used H9 cells infected with the HIV-1_{MN} isolate. Different MAbs were titrated onto cells that had or had not been pretreated with DexS or ATA. As can be seen in Fig. 2, low concentrations of DexS (<100 nM) inhibited the binding of 17b and 48d to the cells by >50%. Interestingly, the CD4bs-specific MAb IgG1b12 was also partially inhibited by DexS, suggesting the occurrence of either polyanion interference with the CD4bs on oligomeric as opposed to monomeric gp120 or DexS-induced dissociation of gp120 from gp41 as has been previously reported (6). The latter explanation seems unlikely to account entirely for the IgG1b12 inhibition, however, since 447-52D binding was only weakly inhibited by DexS at all concentrations tested whereas gp120 dissociation would affect both epitopes in the same way. ATA was also a potent inhibitor of 17b binding but had little effect on IgG1b12 binding at the concentrations used (Fig. 2B). Since ATA does not induce significant gp120 dissociation (unpublished results), this result is consistent with a direct effect of anionic compounds on MAb binding to CD4i epitopes. Levels of CD4i and CD4bs MAb inhibition similar to those obtained in this experiment were observed for cells infected with HIV-1_{HX10} (results not shown).

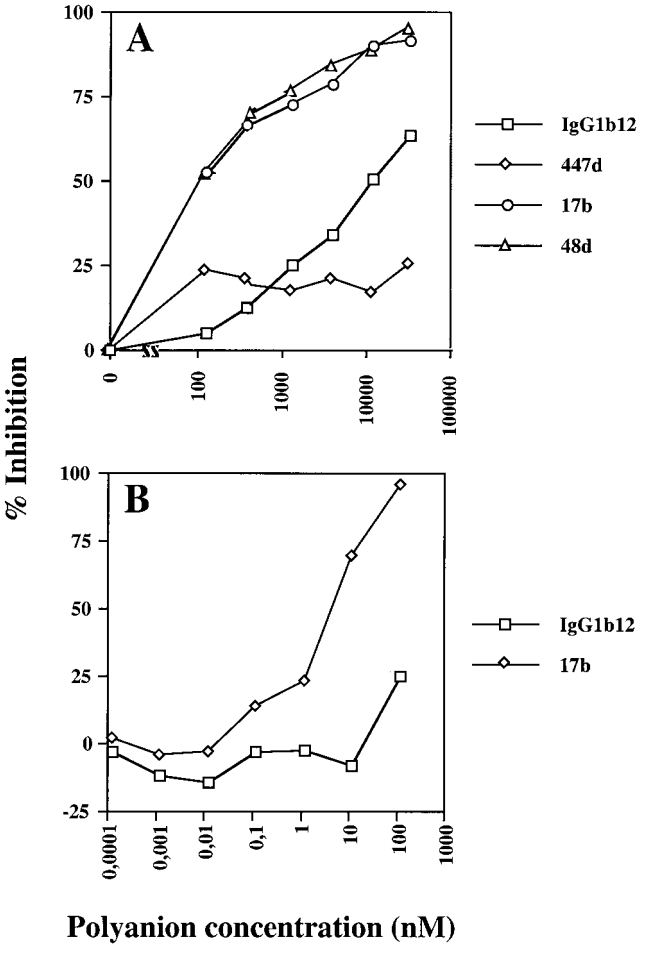

FIG. 2. Inhibition of MAb binding to oligomeric Env expressed on the surface of HIV-1_{MN}-infected cells. Cells were preincubated with various concentrations of DexS (A) or ATA (B) before being washed, and gp120-specific MAbs were added. Bound MAb was detected by indirect immunofluorescence and flow cytometry, and the results are expressed as percent inhibition of MAb binding relative to the positive (no inhibitor) and negative (no MAb) controls. Each datum point is the mean of values for triplicate samples.

DexS interferes with gp120-CXCR4 interactions. We showed previously that the binding of TCLA X4 gp120 to $CD4^+$ $CXCR4^+$ cells inhibited the binding of the CXCR4-specific MAb 12G5, demonstrating a CD4-dependent interaction between gp120 and CXCR4 (49, 84). The observation that DexS could associate with the V3 loop and conserved chemokine binding surface of gp120 implied that polyanions would interfere with gp120-coreceptor interactions. To test this, we attempted to block the inhibition of CXCR4-specific MAb binding by sgp120 at the surface of $CD4^+$ $CXCR4^+$ cells by pretreating the sgp120 with polyanions prior to incubation with the cells. The attachment of sgp120 to CD4 was monitored indirectly by measuring the inhibition of binding of a CD4 MAb (Q4120) that competes with gp120 for CD4 binding (49, 84). Incubation of the cells with $gp120_{MN}$ inhibited 12G5 binding by approximately 35% (data not shown). Increasing concentrations of DexS reduced the inhibition of CXCR4 MAb 12G5 binding to the cells to a maximum of about 80% at 6.6 μM, suggesting that the polyanion was interfering with the gp120-CXCR4 interaction (Fig. 3A). We excluded the possibility of any effects of DexS on the binding of gp120 to CD4 by demonstrating that Q4120 inhibition was essentially complete

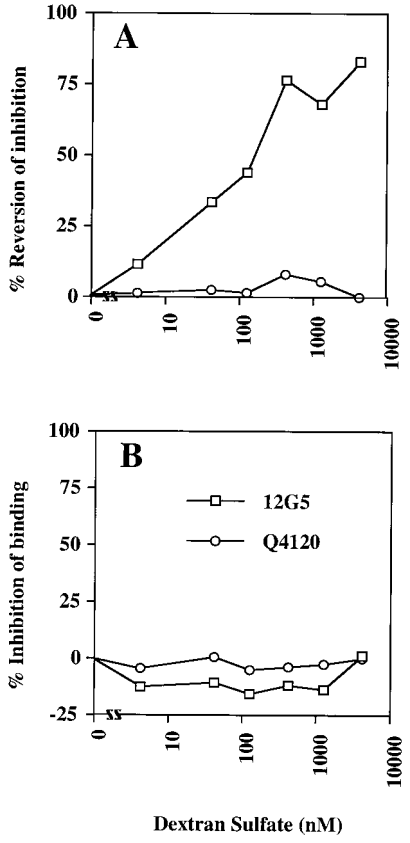

FIG. 3. DexS inhibition of gp120-CXCR4 interactions. (A) A3.01 ($CD4^+$ $CXCR4^+$) T cells were preincubated with various concentrations of DexS prior to the addition of HIV-1_{MN} gp120. The CXCR4-specific MAb 12G5 or the CD4-specific MAb Q4120 was subsequently added. (B) A3.01 cells were preincubated with DexS prior to addition of MAb 12G5 or Q4120. Bound MAb was detected by indirect immunofluorescence and flow cytometry, and the results are expressed as percent inhibition of MAb binding relative to the positive (no inhibitor) and negative (no MAb) controls. Each datum point is the mean of values obtained from triplicate samples.

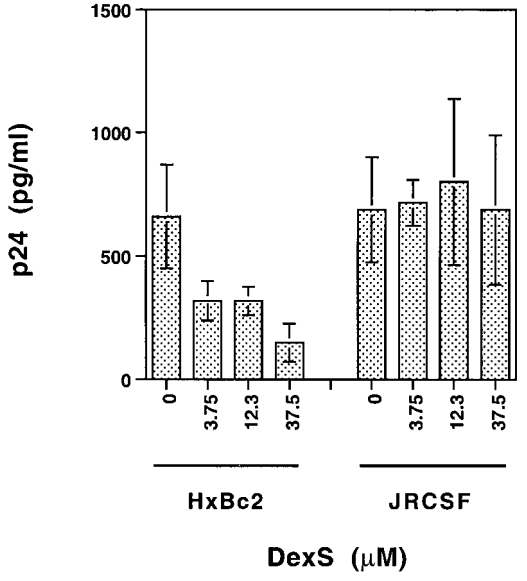

FIG. 4. Inhibition of HIV-1 infectivity by DexS. HIV-1_{HXBc2} and HIV-1_{JRCSF} were preincubated for 1 h at 37°C with the concentrations of DexS shown, then added to activated PBL for a further 1 h. After being washed, the cells were cultured for 7 days, and then the production of virus was measured by detection of cell-free viral p24 in the supernatant. The results, expressed as picograms of p24 per milliliter, were calculated from the optical densities at 492 nm. Each bar represents the mean of values for three replicate wells, and the error bars indicate ± 1 standard deviation.

at all concentrations of DexS used, and we eliminated the possibility that DexS inhibited the binding of 12G5 or Q4120 to CXCR4 and CD4, respectively, by preincubating the cells and MAbs directly with DexS in the absence of gp120 (Fig. 3B).

Selective inhibition of X4 virus infectivity by DexS. To determine whether the ability of polyanions to selectively bind basic gp120 molecules correlated with inhibition of viral infectivity, we tested the effect of DexS on the infection of activated PBL by HIV-1_{HXBc2} (X4 TCLA) and HIV-1_{JRCSF} (R5 PI). Equivalent infectious doses of each virus were preincubated with various concentrations of DexS and then incubated with phytohemagglutinin-activated PBL for 2 h. The cells were subsequently washed thoroughly, to prevent inhibition of viral infectivity at steps subsequent to virus binding and entry, and cultured for 7 days. Infectivity was assayed by detection of cell-free HIV-1 p24. Figure 4 shows that the HXBc2 titer was reduced in a dose-dependent manner from 0.66 ng/ml in the absence of DexS to 0.15 ng/ml in the presence of 37.5 nM DexS (a 77% reduction in infectivity), whereas the titer of JRCSF remained constant, at about 0.7 ng/ml, regardless of the presence of DexS. Thus, X4 HIV-1 appears to be considerably more susceptible to DexS inhibition than is R5 HIV-1, coordinate with the results of polyanion binding to gp120 (see below).

Binding of [^{35}S]heparin to WT and mutated forms of sgp120. The inhibition of CD4i-specific MAb binding to sgp120 by polyanions may be the result of direct competition for MAb binding to the epitope cluster or of indirect effects, such as steric inhibition resulting from polyanion attachment to the V3 loop or polyanion-induced conformational changes in the MAb epitopes. In an attempt to discriminate between these different possibilities, we measured the binding of ^{35}S-labeled heparin to WT and mutated forms of sgp120 lacking the V3 loop. Initial experiments established that [^{35}S]heparin bound X4 sgp120 in a dose-dependent and saturable manner and that unlabeled heparin could efficiently compete with the labeled heparin for binding sites (results not shown). Incubation of WT HXBc2 with [^{35}S]heparin under the above-described conditions resulted in a signal-to-noise ratio of about 40-fold (Fig. 5A). Deletion of the V3 loop resulted in a dramatic decrease in heparin binding (~12-fold). By contrast, $gp120_{JRFL}$bound [^{35}S]heparin only weakly (about twice the background level), and deletion of the V3 loop resulted in a reduction of [^{35}S]heparin binding to close to background levels. These data suggest that the V3 loop of X4 gp120 is an important determinant of polyanion binding but imply that other regions also contribute, albeit to a lesser extent. To address which other regions of X4 gp120 might be implicated in polyanion binding, we tested $gp120_{HXBc2}$ molecules with more-substantial deletions and attempted to inhibit [^{35}S]heparin binding with MAb 48d, which is specific for the CD4i epitope. In this experiment, the level of [^{35}S]heparin binding to WT $gp120_{HXBc2}$ was about ninefold higher than the background (Fig. 5B). Preincubation of WT $gp120_{HXBc2}$ with 48d resulted in a modest but significant decrease in [^{35}S]heparin binding. Deletion of the NH_2 and COOH termini and the V1/V2 loop structure ($HXBc2_{\Delta 82\Delta C5\Delta V1V2}$) resulted in a similarly small decrease in [^{35}S]heparin binding, and preincubation of this mutant with MAb 48d reduced the signal further.

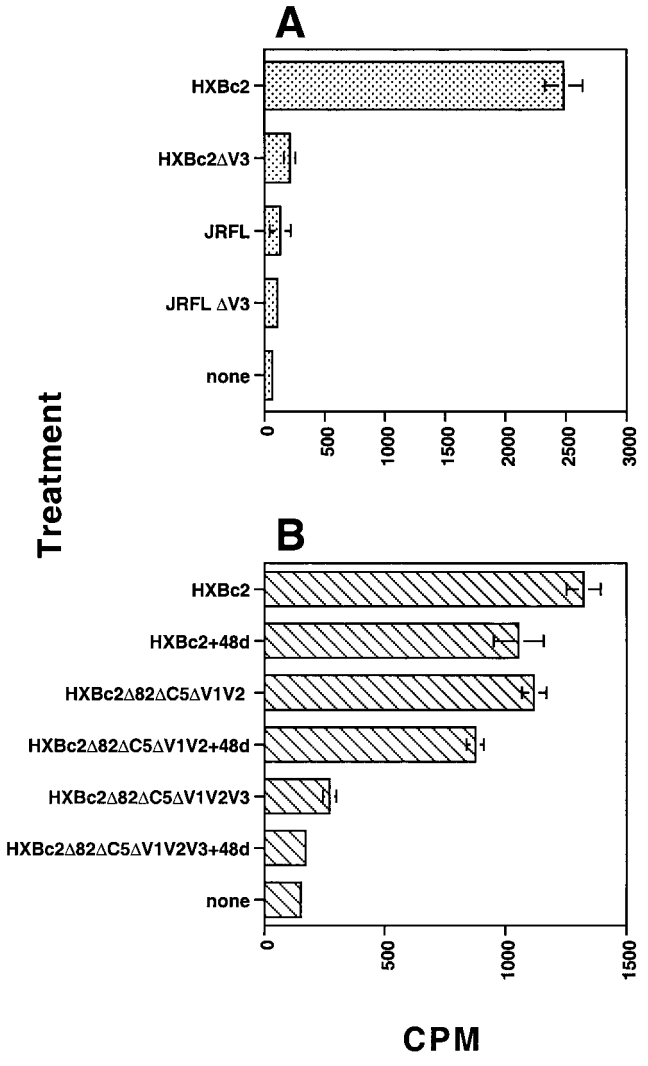

FIG. 5. Direct binding of [^{35}S]heparin to immobilized gp120. gp120 and mutated forms thereof were incubated with [^{35}S]heparin before being blotted onto a nitrocellulose membrane. The radioactivity in bound material was determined with a scintillation counter, and results are expressed as counts per minute. (A) Binding of [^{35}S]heparin to 400 nM $gp120_{HXBc2}$, $gp120_{JRFL}$, and V3 loop deletion mutants thereof. (B) Binding of [^{35}S]heparin to 170 nM $gp120_{HXBc2}$, and mutants thereof, precomplexed (or not) with a molar excess of MAb 48d. The background value for [^{35}S]heparin represents binding to the filter in the absence of protein. Each bar represent the mean of values for triplicate samples, and the error bars represent ± 1 standard deviation.

An additional deletion of the V3 loop ($HXBc2_{\Delta 82\Delta C5\Delta V1V2V3}$) dramatically reduced [^{35}S]heparin binding, and preincubation of this mutant with 48d further reduced binding to background levels. These data suggest that the COOH and NH_2 termini and the V1/V2 loops of HXBc2 gp120 contribute minimally to the attachment of polyanions whereas the V3 loop is the major determinant. Moreover, the inhibition by MAb 48d of [^{35}S]heparin binding to all three forms of gp120 (WT, $HXBc2_{\Delta 82\Delta C5\Delta V1V2}$, and $HXBc2_{\Delta 82\Delta C5\Delta V1V2V3}$) is consistent with [^{35}S]heparin interaction with the conserved chemokine receptor binding surface.

Analysis of the gp120-heparin interaction by SPR. The results obtained in the labeled heparin binding studies suggest that the affinity of heparin for monomeric sgp120 depends on the conservation of the V3 loop and is strongly influenced by the V3 loop charge. However, the binding of soluble polyanions to sgp120 in solution is a poor imitation of the physiological interaction between cell membrane-anchored HSPG and gp120. Thus, we adopted a more physiologically relevant system in which heparin is coupled to the solid phase and sgp120 binding is analyzed by SPR. Not only does this system better represent HSPG presentation at the cell surface, but the multimerization of the heparin-binding sites may increase the avidity for sgp120 if binding occurs at more than one site. Injection of a range of concentrations (up to 45 nM) of X4 $sgp120_{HXBc2}$ over a sensor chip coated with no more than 20 to 25 RU of size-fractionated heparin gave typical sensorgrams (Fig. 6A). Higher densities of heparin were not used on the sensor chip because they gave rise to a mass transport effect that precluded precise kinetic analyses. Preliminary evaluation of the sensorgrams by linear transformation of the primary data indicated that the binding was complex and did not follow single exponential curves. Kinetic analyses were therefore performed by numerical integration, which allows fitting of the data to complex interaction models. Simultaneous fitting to all curves (including both association and dissociation phases), a procedure which improves the robustness of the fitting procedure (54), was carried out by using the Biaeval 3.0 software. Our data could not be fitted to single one-to-one binding as indicated above, and such a model returned a χ^2 value (which describes the closeness of the fit) of 4.25. There are several possible explanations for a value of this magnitude (some of which are inherent to the technology itself [43]), but it is likely that this reflects the existence of a complex binding process (see below). To analyze the gp120-heparin interaction in more detail, we generated data under conditions in which the association phase was allowed to proceed to equilibrium. Equilibrium was reached after 20 min (data not shown), and these data were analyzed to provide an affinity value independently of the kinetic aspect of the binding (Fig. 6B). The overall equilibrium constant was 220 nM, a value considerably lower than the K_d (10 nM) previously determined by direct binding of [^{35}S]heparin to MN gp120 (33). However, these previously performed experiments were carried out in the absence of salt, whereas all of our binding buffers contained a physiological concentration of NaCl (0.15 M), an important point for electrostatic-based interactions (heparin-gp120 binding is completely inhibited by 1 M NaCl, and this concentration was used to regenerate the chip after each gp120 injection). The stochiometry of the binding indicated that on average, 4.4 gp120 molecules bind each heparin chain.

In view of the data presented above (Fig. 1, 2, and 4) which suggest the existence of two distinct heparin binding domains within the gp120 molecule (the V3 loop and the CD4i region), we investigated the possibility that our data could be described by a more complex binding model such as the bivalent analyte model. Using this model, the fitting procedure returned a χ^2 value of 1.5, demonstrating that this model described our data well. The first gp120-heparin binding event was thus characterized by a relatively high on rate, $k_{on}1 = 2.7 \times 10^5\ M^{-1}\ s^{-1}$, and by a rapid dissociation rate constant, $k_{off}1 = 0.147\ s^{-1}$, resulting in an affinity of $K_d = k_{off}1/k_{on}1 = 550$ nM. A second binding event, whose dissociation constant, $k_{off}2$, was $1.58 \times 10^{-3}\ s^{-1}$, further stabilized the complex, yielding the observed affinity. To add support to the existence of two heparin binding sites on gp120, we investigated the effect of prebinding MAbs to sgp120 before reaction with immobilized heparin. In this assay, 45 nmol of gp120 was preincubated with 450 nmol of MAb 50-23 (V3 loop) or MAb 48d (CD4i), either alone or in combination, and then injected over the heparin surface. The results (Fig. 6C) show that a complex made up of gp120 and an

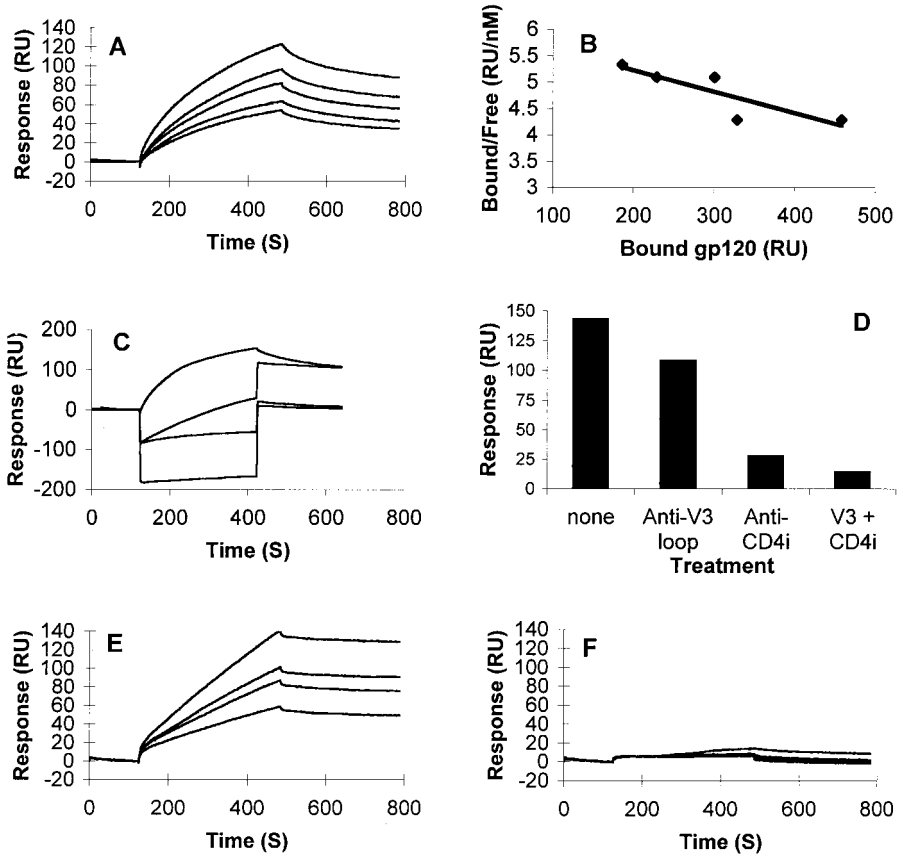

FIG. 6. SPR analysis of X4-derived gp120–heparin interactions: overlay of sensorgrams showing binding of WT and mutated forms of $gp120_{HXBc2}$ to immobilized heparin. sgp120 (used at concentrations of [from top to bottom] 45, 30, 22.5, 15, and 11.5 nM) was injected for 6 min over a heparin-activated surface at a flow rate of 15 μl/min to analyze the association phase, after which running buffer alone was injected to analyze the dissociation phase. (A) Binding curves for wild-type $gp120_{HXBc2}$. (B) Scatchard plot of the equilibrium binding data directly measured on the sensorgrams after a 25-min period of interaction. (C) Binding curves for $gp120_{HXBc2}$, alone or preincubated with a 10-fold molar excess of MAb 50-23, 48d, or both (from top to bottom). (D) Maximum responses measured at the end of the association phases shown in panel C. (E and F) Binding curves for $gp120_{HXBc2\Delta82\Delta C5\Delta V1V2}$ (E) and $gp120_{HXBc2\Delta82\Delta C5\Delta V1V2V3}$ (F) injected at (from top to bottom) 90, 60, 45, and 30 nM over the heparin surface.

anti-V3-loop MAb was still able to bind heparin, supporting the existence of a binding site outside of the 50-23 MAb epitope. Prebinding MAb 48d strongly inhibited the gp120-heparin interaction, consistent with the results obtained in [^{35}S]heparin-gp120 binding studies (Fig. 5B). Finally, a complex of both MAbs with gp120 reduced the heparin-gp120 interaction to close to background levels. The total responses (in RU) at the end of the injections are shown in Fig. 6D. The percentage inhibition caused by MAbs could not be ascertained because the SPR signal is sensitive to mass, and the responses were obtained from different gp120-MAb complexes. However, it is clear from a visual inspection that occupation of both the V3 loop and the CD4i region is required to produce almost complete (>90%) inhibition of gp120-heparin binding.

The mutant $gp120_{HXBc2\Delta N\Delta C\Delta V1V2}$ gave binding curves different from those obtained with the intact molecule; they did not fit any obvious model of ligand-receptor binding, probably as a result of mass transport (Fig. 6E). Although we were unable to determine an affinity constant for this molecule, visual inspection of the curves clearly reveals significant heparin binding. The mutant $gp120_{HXBc2\Delta N\Delta C\Delta V1V2V3}$, from which the V3 loop had been further deleted, did not show any significant heparin binding activity under the conditions used (Fig. 6F), consistent with the idea that the V3 loop is the primary high-affinity binding site on gp120. Increasing the density of heparin on the sensor chip resulted in detectable but weak $gp120_{HXBc2\Delta N\Delta C\Delta V1V2V3}$ binding (results not shown), confirming weak polyanion binding activity in the absence of the V3 loop. We next used the same binding assay to compare the heparin binding activities of two R5X4-derived sgp120s, 89.6 and W61D. Results show that $gp120_{89.6}$ (Fig. 7A), but not $gp120_{W61D}$ (Fig. 7B), interacts significantly with the low-density immobilized heparin. These data suggest that the V3 loop charge alone may not be sufficient to explain the heparin binding activity, since these two gp120s differ by only one unit of charge (89.6 = +7 and W61D = +6). It is likely that the other parameters, such as the conformation of the V3 loop and the charge of regions outside of the V3 loop, also influence heparin binding. Finally, R5 $gp120_{JRFL}$, which was analyzed under the same experimental conditions of low heparin density, did not show significant binding activity (Fig. 7C), and deletion of the V3 loop did not obviously modify this activity (Fig. 7D). Weak binding of R5 $gp120_{JRFL}$ was detected when the protein was injected over a higher-density immobilized heparin, consistent with a very-low-affinity interaction (data not shown).

Electrostatic potential of the conserved coreceptor binding surface and the V3 loop. To better understand the interactions taking place between gp120 and polyanions, we prepared models representing the electrostatic potential on the chemokine

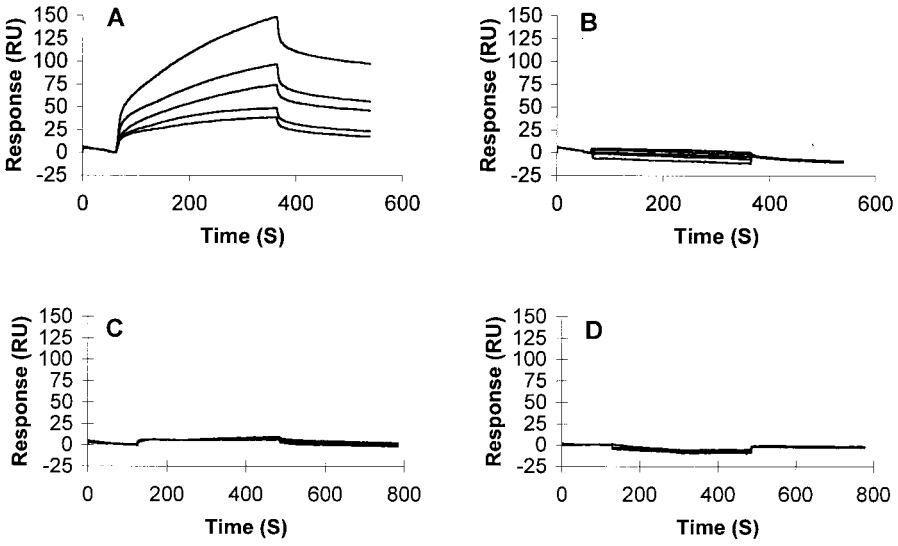

FIG. 7. SPR analysis of R5X4- and R5-derived gp120–heparin interactions: overlay of sensorgrams showing binding of gp120 to immobilized heparin. (A and B) Binding curves for R5X4 $gp120_{89.6}$ (A) and R5X4 $gp120_{W61D}$ (B) injected at (from top to bottom) 60, 45, 30, 22.5, and 15 nM. (C and D) Binding curves for wild-type R5 $gp120_{JRFL}$ (C) and V3 loop-deleted $gp120_{JRFL}$ (D) injected at (from top to bottom) 90, 60, 45, and 30 nM over the heparin surface. Binding conditions were similar to those described in the legend to Fig. 6. S, seconds.

receptor binding surface based on the recently published gp120 core structure. The gp120 cores were modeled as a trimer in a companion paper (45) to give a better indication of the overall charge on this surface, and the V3 loops of gp120 molecules of various origins, modeled as described in that paper (45), were superimposed on the gp120 core structure to illustrate the influence of this loop on the electrostatic potential. Figure 8 shows models oriented with the coreceptor binding surface

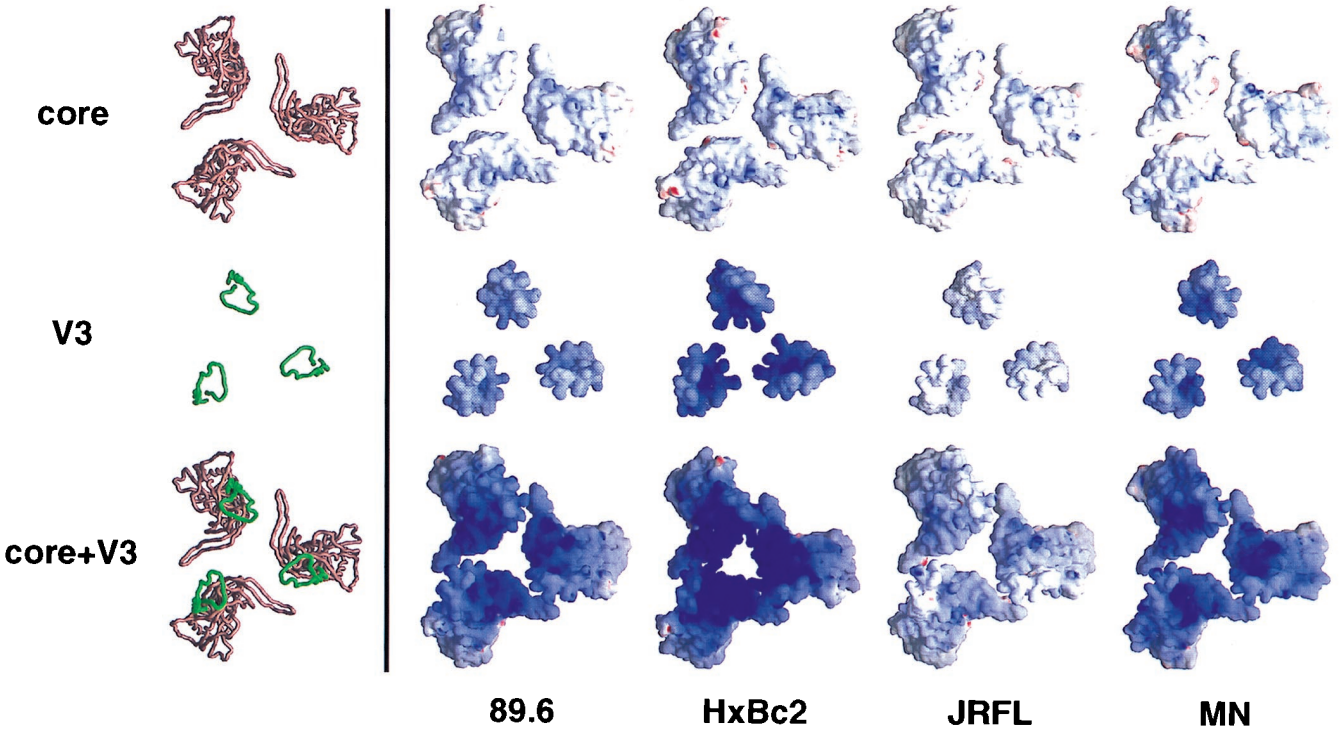

FIG. 8. Modeling of the electrostatic potential for the coreceptor binding surface of the gp120 trimer. The molecular models of the gp120 trimer shown here are orientated with the trimer axis perpendicular to the page, showing the conserved surfaces of the HIV-1 clones HXBc2, MN, 89.6, and JRFL. The top panels show the gp120 core, the middle panels show the V3 loop, and the bottom panels show the V3 loop integrated into the gp120 core. These models are depicted in a Cα worm representation (left column) and an electrostatic surface representation (other four columns). The Cα worm representations for the different strains are essentially indistinguishable: the one corresponding to the HXBc2 sequence is shown with the core colored rust brown and the V3 loop colored green. The electrostatic potentials were calculated with the program Delphi and are depicted at the solvent-accessible surface, which is colored according to the local electrostatic potential, ranging from dark blue (most positive, corresponding to 10 kT/e) to red (most negative). The figure was prepared with the program GRASP (56).

facing out from the page. The top panel represents the electrostatic potential of the $gp120_{HXBc2\Delta N\Delta C\Delta V1V2V3}$ core. The coreceptor binding surface is weakly basic (basic is represented by blue, acidic is represented by red, and neutral is represented by white). Subtle differences are, however, evident in the degree of positivity; the coreceptor binding surface on the gp120 core of HXBc2 is slightly more basic than those of the other gp120s. The middle panel of Fig. 8 represents the electrostatic potential on models of the V3 loops derived from primary *env* sequences of the viruses MN (X4), HXBc2 (X4), 89.6 (R5X4), and JRFL (R5). The HXBc2, MN, and 89.6 V3 loops are highly basic (+9, +8, and +7 charge, respectively), whereas the JRFL V3 loop is relatively weakly basic (+4). The lower panel of Fig. 8 illustrates the overall charge of the coreceptor binding surface with the V3 loop modeled onto the gp120 core. It is clear from these models that the V3 loop charge dominates the electrostatic potential. The spatial overlap of the V3 loop and the conserved coreceptor binding surface observed in the electrostatic model is consistent with the sulfated chains of polyanionic molecules being able to bind both sites.

DISCUSSION

In this study we have demonstrated by several different techniques that polyanions interact with the V3 loop and the newly characterized conserved coreceptor binding surface on gp120 in a manner dependent on viral origin and coreceptor usage. Thus, the monomeric X4 and R5X4 gp120 molecules tested here bind polyanions strongly whereas R5 gp120 binds polyanions relatively weakly ($gp120_{Bal}$) or not at all ($gp120_{JRFL}$). Most of this variation comes from changes in the charge and structure of the V3 loop, but variability in the conserved coreceptor binding surface, which displays some interisolate differences in electrostatic potential (Fig. 8 and results not shown), may also influence polyanion binding. The data that we have obtained from kinetic and MAb inhibition studies of gp120-heparin binding strongly suggest a phenomenon based on an initial high-affinity association via the V3 loop followed by weaker binding via a second site, most probably the conserved coreceptor binding region. Although we do not have unequivocal evidence of a direct interaction between polyanions and the conserved coreceptor binding surface, the data presented here provide a strong case for this. Thus, (i) polyanions potently inhibit the attachment of MAbs specific for the conserved coreceptor binding surface and regions of the V3 loop but, with the exception of one V2 loop-specific MAb, have little or no effect on MAbs to other exposed regions of gp120; (ii) CD4i-specific and V3 loop-specific MAbs inhibit the heparin-gp120 interaction in an additive manner; (iii) heparin binds mutants of gp120 from which the NH_2 and COOH termini and the variable loops V1, V2, and V3 have been deleted, and the CD4i MAb 48d interferes with the binding of heparin to this mutant; and (iv) weak binding of heparin to $gp120_{HXBc2\Delta V3}$, $gp120_{JRFL\Delta V3}$, and $gp120_{HXBc2\Delta 82\Delta C5\Delta V1V2V3}$ can be observed under the appropriate conditions.

The molecular model of the electrostatic potential on the coreceptor-binding face of gp120 shows that the basic nature of the combined V3 loop-conserved coreceptor binding surface is dominated by the V3 loop charge. Although the models presented here and in reference 45 are of low resolution, it is clear that relatively long-chain sulfated polysaccharides such as heparin would be capable of spanning the V3 loop and the conserved coreceptor binding surface, which exhibit considerable spatial overlap. Moreover, several molecules of gp120 could bind a single heparin chain. V3 loop charge and conformation (12, 14, 60, 73, 85), in association with the variable loops V1 and V2 (11, 46, 67, 72), determine coreceptor usage and viral tropism in vitro. It seems likely, based on our current understanding of HIV-1 attachment to receptor-bearing cells, that polyanion binding to gp120 parallels, at least to some extent, the interaction between gp120 and its coreceptors. Binding of gp120 to the appropriate coreceptor is thought to take place initially via the V3 loop, an interaction that determines coreceptor-gp120 specificity (12, 14, 38, 92), followed by exposure and binding of the conserved coreceptor binding region (64, 78, 87). The importance of electrostatic interactions in the gp120-coreceptor association is underscored by a series of studies that demonstrate a reduction in gp120-CCR5 binding and coreceptor function in virus infectivity and fusion assays following substitution of acidic or potentially sulfated amino acids in the amino terminus of CCR5 (21, 23, 24, 62). However, interactions other than those mediated by the chemokine receptor NH_2 terminus are also required for virus fusion to be fully activated, such as those based around the second extracellular loops of CCR5 (20) and CXCR4 (5).

There is no direct evidence for HIV-1 adaptation to HSPG use in vivo; the evolution of the V3 loop toward a more basic structure appears to come from adaptation to CXCR4 usage (70). However, adaptation of HIV-1 to replicate in T-cell lines in vitro may be driven, at least in part, by increased interaction between the V3 loop and cell surface HSPG, since human T-lymphotropic leukemia virus type 1-immortalized T-cell lines such as H9, MT-2, and c8166 that have been used routinely to isolate, propogate, and phenotype viruses from infected individuals express large amounts of surface HSPG (57). Indeed, this may help to explain why viruses passaged only in primary cells such as activated $CD4^+$ T cells and macrophages, which express only small amounts of HSPG (40, 57, 58), do not have V3 loops with net positive charges greater than +5 or +6 whereas viruses passaged in immortalized cell lines that express high levels of HSPG frequently have very basic V3 loops with net positive charges of +8 and +9 (28, 42). In the present study, analysis of X4 gp120 was carried out with TCLA virus-derived clones. Clearly, further studies of PI X4 virus-derived sgp120 will have to be done as this becomes available. However, the finding that the R5X4 PI gp120 89.6 binds heparin implies that PI X4 virus sgp120 will have a similar phenotype.

Although HIV-1 may use HSPG as a low-affinity attachment receptor, allowing the virus to scan the cell surface for specific entry receptors (34, 83), the biological implications of gp120 binding to HSPG are unclear, since the principal target cells for HIV-1 in vivo, $CD4^+$ T cells and macrophages, have little HSPG on their surfaces. Nevertheless, even low levels of HSPG influence the efficiency of viral attachment and therefore entry and so may have important consequences for infectivity and cellular tropism in vivo. A selective ability of X4 and R5X4 viruses to attach to these cells via HSPG may give these viruses an advantage over R5 viruses that are potentially less able to do so. Other cell types that carry large amounts of HSPG are endothelial and epithelial cells (50), and certain tissues, such as the liver, are very rich in HSPG expression (66). These cell and tissue types are considered to be nonpermissive for HIV infection, but one potential consequence of HSPG expression may be the preferential trapping of X4 and R5X4 viruses onto their surfaces, leading to selective exhaustion of these viral phenotypes in vivo (83). Such a phenomenon may help to explain the preferential transmission and early dominance of R5 viruses over R5X4 and X4 viruses in vivo.

Our observation that polyanions bind recombinant, monomeric sgp120 was reproduced with oligomeric, gp41-associated forms of X4 gp120 expressed on HIV-1-infected cells, suggesting that the monomeric form may represent to some extent the

functional heterotrimeric form of gp120. However, it is very likely that the trimeric form will have a greater avidity for membrane HSPG complexes. Experimental evidence supporting this comes from a study by Roderiquez et al. (65), who demonstrated that whereas no binding of monomeric TCLA X4 gp120 to cell surface HSPG was detectable, oligomeric TCLA X4 gp140 derived from the same isolate bound specifically. Thus, the 220 nM affinity constant observed for monomeric $sgp120_{HXBc2}$ binding to immobilized heparin may be of high avidity when multiple interactions of this type take place on the surface of a virion. This idea is consistent with the predicted occupation of four or five molecules of gp120 by one heparin chain under our experimental conditions. Moreover, although we observed only a weak association between soluble or immobilized polyanions and monomeric R5 sgp120, the interaction with oligomeric gp120, either soluble or virion associated, could be stronger, as predicted by the electrostatic properties of the gp120 trimer. Future studies will need to address the kinetics of binding of oligomeric gp140 or whole virus particles to immobilized heparin or membrane HSPG.

The use of polyanionic compounds such as DexS as anti-HIV therapeutic agents systemically has not had obvious success in clinical trials, since there has been no obvious benefit to the patients (1, 26), adsorption has been considered poor (47), and some toxicity has been observed (26). However, other studies are more optimistic with regard to the use of polyanionic compounds as anti-HIV and antiviral therapeutic agents either systemically (30, 36) or locally (74). One reason for the failure of these molecules in vivo may be their weak neutralization activity for R5 viruses (Fig. 4), the viral phenotype associated with HIV-1 transmission and early infection. Another is that HIV variants resistant to DexS inhibition are rapidly generated in vitro, suggesting that similar events would occur in vivo (22). However, the finding that the basic and highly conserved coreceptor binding region interacts with polyanions and the recent availability of the gp120 core crystal structure may allow for novel strategies in the rational development of small-molecule inhibitors of X4 and perhaps R5 HIV-1 infection based on electrostatic interactions with gp120.

ACKNOWLEDGMENTS

We thank H. Holmes and the MRC AIDS Reagent Repository for supplying reagents and D. Burton, J. Robinson, J. Gershoni, G. Denisova, and S. Zolla-Pazner for kind gifts of monoclonal antibodies.

This study was supported by the Centre National de la Recherche Scientifique, the Institut National de la Santé et la Recherche Médicale, the Agence Nationale de Recherches sur le SIDA, the Fondation pour la Recherche Médicale (SIDACTION), and the European Community Biomed II shared cost action "Antibody Mediated Enhancement and Neutralization of Lentivirus Infections: Role in Immune Pathogenesis and Vaccine Development." P.D.K. was a recipient of a Burroughs Wellcome career development award, and M.M. was the recipient of a Philipps Foundation Fellowship.

REFERENCES

1. **Abrams, D. I., S. Kuno, R. Wong, K. Jeffords, M. Nash, J. B. Molaghan, R. Gorter, and R. Ueno.** 1989. Oral dextran sulfate (UA001) in the treatment of the acquired immunodeficiency syndrome (AIDS) and AIDS-related complex. Ann. Intern. Med. **110:**183–188.
2. **Bagasra, O., and H. W. Lischner.** 1988. Activity of dextran sulfate and other polysaccharides against human immunodeficiency virus. J. Infect. Dis. **158:** 1084–1087.
3. **Batinic, D., and F. A. Robey.** 1992. The V3 region of the envelope glycoprotein of human immunodeficiency virus type 1 binds sulfated polysaccharides and CD4-derived synthetic peptides. J. Biol. Chem. **267:**6664–6671.
4. **Berger, E. A., R. W. Doms, E.-M. Fenyo, B. T. M. Korber, D. R. Littman, J. P. Moore, Q. J. Sattentau, H. Schuitemaker, J. Sodroski, and R. A. Weiss.** 1997. HIV-1 phenotypes classified by co-receptor usage. Nature **391:**240.
5. **Brelot, A., N. Heveker, O. Pleskoff, N. Sol, and M. Alizon.** 1997. Role of the first and third extracellular domains of CXCR-4 in human immunodeficiency virus coreceptor activity. J. Virol. **71:**4744–4751.
6. **Bugelski, P. J., H. Ellens, T. K. Hart, and R. L. Kirsh.** 1991. Soluble CD4 and dextran sulfate mediate release of gp120 from HIV-1: implications for clinical trials. J. Acquir. Immune Defic. Syndr. **4:**923–924.
7. **Burton, D. R., J. Pyati, R. Koduri, S. J. Sharp, G. B. Thornton, P. W. Parren, L. S. Sawyer, R. M. Hendry, N. Dunlop, P. L. Nara, and D. Burton.** 1994. Efficient neutralization of primary isolates of HIV-1 by a recombinant human monoclonal antibody. Science **266:**1024–1027.
8. **Callahan, L. N., M. Phelan, M. Mallinson, and M. A. Norcross.** 1991. Dextran sulfate blocks antibody binding to the principal neutralizing domain of human immunodeficiency virus type 1 without interfering with gp120-CD4 interactions. J. Virol. **65:**1543–1550.
9. **Catasti, P., J. D. Fontenot, E. M. Bradbury, and G. Gupta.** 1995. Local and global structural properties of the HIV-MN V3 loop. J. Biol. Chem. **270:** 2224–2232.
10. **Chen, Y., T. Maguire, R. E. Hileman, J. R. Fromm, J. D. Esko, R. J. Linhardt, and R. M. Marks.** 1997. Dengue virus infectivity depends on envelope protein binding to target cell heparan sulfate. Nat. Med. **3:**866–871.
11. **Cho, M. W., M. K. Lee, M. C. Carney, J. F. Berson, R. W. Doms, and M. A. Martin.** 1998. Identification of determinants on a dualtropic human immunodeficiency virus type 1 envelope glycoprotein that confer usage of CXCR4. J. Virol. **72:**2509–2515.
12. **Choe, H., M. Farzan, Y. Sun, N. Sullivan, B. Rollins, P. D. Ponath, L. Wu, C. R. Mackay, G. LaRosa, W. Newman, N. Gerard, C. Gerard, and J. Sodroski.** 1996. The β-chemokine receptors CCR3 and CCR5 facilitate infection by primary HIV-1 isolates. Cell **85:**1135–1148.
13. **Chung, C.-S., J.-C. Hsiao, Y.-S. Chang, and W. Chang.** 1998. A27L protein mediates vaccinia virus interaction with cell surface heparan sulfate. J. Virol. **72:**1577–1585.
14. **Cocchi, F., A. L. DeVico, A. Garzino-Demo, A. Cara, R. C. Gallo, and P. Lusso.** 1996. The V3 domain of the HIV-1 gp120 envelope glycoprotein is critical for chemokine-mediated blockade of infection. Nat. Med. **2:**1244–1247.
15. **Conley, A. J., M. K. Gorny, J. A. Kessler II, L. J. Boots, M. Ossorio-Castro, S. Koenig, D. W. Lineberger, E. A. Emini, C. Williams, and S. Zolla-Pazner.** 1994. Neutralization of primary human immunodeficiency virus type 1 isolates by the broadly reactive anti-V3 monoclonal antibody, 447-52D. J. Virol. **68:**6994–7000.
16. **Deen, K. C., J. S. McDougal, R. Inacker, G. Folena-Wasserman, J. Arthos, J. Rosenberg, P. J. Maddon, R. Axel, and R. W. Sweet.** 1988. A soluble form of CD4 (T4) protein inhibits AIDS virus infection. Nature **331:**82–84.
17. **Dimitrov, D. S., and C. C. Broder.** 1997. HIV and membrane receptors. Landes Bioscience, Austin, Tex.
18. **Ditzel, H. J., P. W. H. I. Parren, J. Binley, J. Sodroski, J. P. Moore, C. F. Barbas, and D. R. Burton.** 1997. Mapping the protein surface of HIV-1 gp120 using human monoclonal antibodies from phage display libraries. J. Mol. Biol. **267:**684–689.
19. **Doms, R. W., A. L. Edinger, and J. P. Moore.** 1998. Coreceptor use by primate lentiviruses. Los Alamos National Laboratory, Los Alamos, N.Mex.
20. **Doms, R. W., and S. C. Peiper.** 1997. Unwelcomed guests with master keys: how HIV uses chemokine receptors for cellular entry. Virology **235:**179–190.
21. **Dragic, T., A. Trkola, S. W. Lin, K. A. Nagashima, F. Kajumo, L. Zhao, W. C. Olson, L. Wu, C. R. Mackay, G. P. Allaway, T. P. Sakmar, J. P. Moore, and P. J. Maddon.** 1998. Amino-terminal substitutions in the CCR5 coreceptor impair gp120 binding and human immunodeficiency virus type 1 entry. J. Virol. **72:**279–285.
22. **Este, J. A., D. Schols, K. De Vreese, K. Van Laethem, A. M. Vandamme, J. Desmyter, and E. De Clercq.** 1997. Development of resistance of human immunodeficiency virus type 1 to dextran sulfate associated with the emergence of specific mutations in the envelope gp120 glycoprotein. Mol. Pharmacol. **52:**98–104.
23. **Farzan, M., H. Choe, L. Vaca, K. Martin, Y. Sun, E. Desjardins, N. Ruffing, L. Wu, R. Wyatt, N. Gerard, C. Gerard, and J. Sodroski.** 1998. A tyrosine-rich region in the N terminus of CCR5 is important for human immunodeficiency virus type 1 entry and mediates an association between gp120 and CCR5. J. Virol. **72:**1160–1164.
24. **Farzan, M., T. Mirzabekov, P. Kolchinsky, R. Wyatt, M. Cayabyab, N. P. Gerard, C. Gerard, J. Sodroski, and H. Choe.** 1999. Tyrosine sulfation of the amino terminus of CCR5 facilitates HIV-1 entry. Cell **96:**667–676.
25. **Fisher, A. G., B. Ensoli, D. Looney, A. Rose, R. C. Gallo, M. S. Saag, G. M. Shaw, et al.** 1988. Biologically diverse molecular variants within a single HIV-1 isolate. Nature **334:**444–447.
26. **Flexner, C., P. A. Barditch-Crovo, D. M. Kornhauser, H. Farzadegan, L. J. Nerhood, R. E. Chaisson, K. M. Bell, K. J. Lorentsen, C. W. Hendrix, B. G. Petty, and P. S. Lietman.** 1991. Pharmacokinetics, toxicity, and activity of intravenous dextran sulfate in human immunodeficiency virus infection. Antimicrob. Agents Chemother. **35:**2544–2550.
27. **Flynn, S. J., and P. Ryan.** 1995. A heterologous heparin-binding domain can promote functional attachment of a pseudorabies virus gC mutant to cell surfaces. J. Virol. **69:**834–839.
28. **Fouchier, R. A. M., M. Groenink, N. A. Kootstra, M. Tersmette, H. G.**

Huisman, F. Miedema, and H. Schuitemaker. 1992. Phenotype-associated sequence variation in the third variable domain of the human immunodeficiency virus type 1 gp120 molecule. J. Virol. **66:**3183–3187.
29. **Fry, E. E., S. M. Lea, T. Jackson, J. W. I. Newman, F. M. Ellard, W. E. Blakemore, R. Abu-Ghazaleh, A. Samuel, A. M. Q. King, and D. I. Stuart.** 1999. The structure and function of a foot and mouth disease virus-oligosaccharide receptor complex. EMBO J. **18:**543–554.
30. **Gordon, M., S. Deeks, C. De Marzo, J. Goodgame, M. Guralnik, W. Lang, T. Mimura, D. Pearce, and Y. Kaneko.** 1997. Curdlan sulfate (CRDS) in a 21-day intravenous tolerance study in human immunodeficiency virus (HIV) and cytomegalovirus (CMV) infected patients: indication of anti-CMV activity with low toxicity. J. Med. **28:**108–128.
31. **Gorny, M. K., A. J. Conley, S. Karwowska, A. Buchbinder, J.-Y. Xu, E. A. Emini, S. Koenig, and S. Zolla-Pazner.** 1992. Neutralization of diverse human immunodeficiency virus type 1 variants by an anti-V3 human monoclonal antibody. J. Virol. **66:**7538–7542.
32. **Harrop, H. A., D. R. Coombe, and C. C. Rider.** 1994. Heparin specifically inhibits binding of V3 loop antibodies to HIV-1 gp120, an effect potentiated by CD4 binding. AIDS **8:**183–192.
33. **Harrop, H. A., and C. C. Rider.** 1998. Heparin and its derivatives bind to HIV-1 recombinant envelope glycoproteins, rather than to recombinant HIV-1 receptor, CD4. Glycobiology **8:**131–137.
34. **Haywood, A. M.** 1994. Virus receptors: binding, adhesion strengthening, and changes in viral structure. J. Virol. **68:**1–5.
35. **Healey, D., L. Dianda, J. P. Moore, J. S. McDougal, M. J. Moore, P. Estess, D. Buck, P. D. Kwong, P. C. L. Beverley, and Q. J. Sattentau.** 1990. Novel anti-CD4 monoclonal antibodies separate human immunodeficiency virus infection and fusion of $CD4^+$ cells from virus binding. J. Exp. Med. **172:** 1233–1242.
36. **Hiebert, L. M., S. M. Wice, L. B. Jaques, K. E. Williams, and J. M. Conly.** 1999. Orally administered dextran sulfate is absorbed in HIV-positive individuals. J. Lab. Clin. Med. **133:**161–170.
37. **Hoffman, T. L., and R. W. Doms.** 1999. HIV-1 envelope determinants for cell tropism and chemokine receptor use. Mol. Membr. Biol. **16:**57–65.
38. **Hoffman, T. L., C. C. LaBranche, W. Zhang, G. Canziani, J. Robinson, I. Chaiken, J. A. Hoxie, and R. W. Doms.** 1999. Stable exposure of the coreceptor-binding site in a CD4-independent HIV-1 envelope protein. Proc. Natl. Acad. Sci. USA **96:**6359–6364.
39. **Honig, B., and A. Nicholls.** 1995. Classical electrostatics in biology and chemistry. Science **268:**1144–1149.
40. **Ibrahim, J., P. Griffin, D. R. Coombe, C. C. Rider, and W. James.** 1999. Cell-surface heparan sulfate facilitates human immunodeficiency virus type 1 entry into some cell lines but not primary lymphocytes. Virus Res. **60:**159–169.
41. **Ito, M., M. Baba, A. Sato, R. Pauwels, E. de Clercq, and S. Shigeta.** 1987. Inhibitory effect of dextran sulfate and heparin on the replication of human immunodeficiency virus (HIV) in vitro. Antivir. Res. **7:**361–367.
42. **Jiang, S.** 1997. HIV-1-coreceptor binding. Nat. Med. **3:**367–368.
43. **Karlson, R., H. Roos, L. Fagerstam, and B. Persson.** 1994. Kinetic and concentration analysis using BIA technology. Methods **6:**99–110.
44. **Kwong, P. D., R. Wyatt, J. Robinson, R. W. Sweet, J. Sodroski, and W. A. Hendrickson.** 1998. Structure of an HIV gp120 envelope glycoprotein in complex with the CD4 receptor and a neutralizing human antibody. Nature **393:**648–659.
45. **Kwong, P. D., R. Wyatt, Q. J. Sattentau, J. Sodroski, and W. A. Hendrickson.** 2000. Oligomeric modeling and electrostatic analysis of the gp120 envelope glycoprotein of human immunodeficiency virus. J. Virol. **74:**1961–1972.
46. **Lee, M. K., J. Heaton, and M. W. Cho.** 1999. Identification of determinants of interaction between CXCR4 and gp120 of a dual-tropic HIV-1DH12 isolate. Virology **257:**290–296.
47. **Lorentsen, K. J., C. W. Hendrix, J. M. Collins, D. M. Kornhauser, B. G. Petty, R. W. Klecker, C. Flexner, R. H. Eckel, and P. S. Lietman.** 1989. Dextran sulfate is poorly absorbed after oral administration. Ann. Intern. Med. **111:**561–566.
48. **Mitsuya, H., D. J. Looney, S. Kuno, R. Ueno, F. Wong-Staal, and S. Broder.** 1998. Dextran sulfate suppression of viruses in the HIV family: inhibition of virion binding to $CD4^+$ cells. Science **240:**646–649.
49. **Mondor, I., M. Moulard, S. Ugolini, P.-J. Klasse, J. Hoxie, R. Wyatt, J. Sodroski, and Q. J. Sattentau.** 1998. Interactions among HIV gp120, CD4, and CXCR4: dependence on CD4 expression level, gp120 viral origin, conservation of the gp120 COOH- and NH_2-termini and V1/V2 and V3 loops, and sensitivity to neutralizing antibodies. Virology **248:**394–405.
50. **Mondor, I., S. Ugolini, and Q. J. Sattentau.** 1998. Human immunodeficiency virus type 1 attachment to HeLa CD4 cells is CD4-independent and gp120 dependent and requires cell surface heparans. J. Virol. **72:**3623–3634.
51. **Moore, J. P., J. A. McKeating, R. A. Weiss, and Q. J. Sattentau.** 1990. Dissociation of gp120 from HIV-1 virions induced by soluble CD4. Science **250:**1139–1142.
52. **Moore, J. P., Q. J. Sattentau, R. Wyatt, and J. Sodroski.** 1994. Probing the structure of the human immunodeficiency virus surface glycoprotein gp120 with a panel of monoclonal antibodies. J. Virol. **68:**469–484.
53. **Moore, J. P., A. Trkola, B. Korber, L. J. Boots, J. A. Kessler II, F. E. McCutchan, J. Mascola, D. D. Ho, J. Robinson, and A. J. Conley.** 1995. A human monoclonal antibody to a complex epitope in the V3 region of gp120 of human immunodeficiency virus type 1 has broad reactivity within and outside clade B. J. Virol. **69:**122–130.
54. **Morton, T. A., D. G. Myszka, and I. M. Chaiken.** 1995. Interpreting complex binding kinetics from optical biosensors: a comparison of analysis by linearization, the integration rate equation, and numerical integration. Anal. Biochem. **227:**176–185.
55. **Nicholls, A., and B. Honig.** 1991. A rapid finite difference algorithm, utilizing successive over-relaxation to solve the Poisson-Boltzmann equation. J. Comput. Chem. **12:**435–445.
56. **Nicholls, A., K. A. Sharp, and B. Honig.** 1991. Protein folding and association: insight from the interfacial and thermodynamic properties of hydrocarbons. Proteins Struct. Funct. Genet. **11:**281–296.
57. **Ohshiro, Y., T. Murakami, K. Matsuda, K. Nishioka, K. Yoshida, and N. Yamamoto.** 1996. Role of cell surface glycosaminoglycans of human T cells in human immunodeficiency virus type 1 (HIV-1) infection. Microbiol. Immunol. **40:**827–835.
58. **Oravecz, T., M. Pall, and M. A. Norcross.** 1996. β-Chemokine inhibition of monocytotropic HIV-1 infection. J. Immunol. **157:**1329–1332.
59. **Patel, M., M. Yanagishita, G. Roderiquez, D. C. Bou-Habib, T. Oravecz, V. C. Hascall, and M. A. Norcross.** 1993. Cell-surface heparan sulfate proteoglycan mediates HIV-1 infection of T-cell lines. AIDS Res. Hum. Retrovir. **9:**167–174.
60. **Pleskoff, O., N. Sol, B. Labrosse, and M. Alizon.** 1997. Human immunodeficiency virus strains differ in their ability to infect $CD4^+$ cells expressing the rat homolog of CXCR-4 (fusin). J. Virol. **71:**3259–3262.
61. **Prince, A. M., B. Horowitz, L. Baker, R. W. Schulman, H. Ralph, J. Valinski, A. Cundell, B. Brotman, W. Boehle, F. Rey, M. Piet, H. Reesink, N. Lelie, M. Tersmette, L. Barbosa, G. Nemo, C. L. Nastala, J. S. Allan, D. R. Lee, and J. W. Eichberg.** 1988. Failure of a human immunodeficiency virus (HIV) immune globulin to protect chimpanzees against experimental challenge with HIV. Proc. Natl. Acad. Sci. USA **85:**6944–6948.
62. **Rabut, G. E. E., J. A. Konner, F. Kajumo, J. P. Moore, and T. Dragic.** 1998. Alanine substitutions of polar and nonpolar residues in the amino-terminal domain of CCR5 differently impair entry of macrophage- and dualtropic isolates of human immunodeficiency virus type 1. J. Virol. **72:**3464–3468.
63. **Rider, C. C., D. R. Coombe, H. A. Harrop, E. F. Hounsell, C. Bauer, J. Feeney, B. Mulloy, N. Mahmood, A. Hay, and C. Parish.** 1994. Anti-HIV-1 activity of chemically modified heparins: correlation between binding to the V3 loop of gp120 and inhibition of cellular HIV-1 infection in vitro. Biochemistry **33:**6974–6980.
64. **Rizzuto, C. D., R. Wyatt, N. Hernandez-Ramos, Y. Sun, P. D. Kwong, W. A. Hendrickson, and J. Sodroski.** 1998. A conserved HIV gp120 glycoprotein structure involved in chemokine receptor binding. Science **280:**1763–1767.
65. **Roderiquez, G., T. Oravecz, M. Yanagishita, D. C. Bou-Habib, H. Mostowski, and M. A. Norcross.** 1995. Mediation of human immunodeficiency virus type 1 binding by interaction of cell surface heparan sulfate proteoglycans with the V3 region of envelope gp120-gp41. J. Virol. **69:**2233–2239.
66. **Roskams, T., H. Moshage, R. De Vos, D. Guido, P. Yap, and V. Desmet.** 1995. Heparan sulfate proteoglycan expression in normal human liver. Hepatology **21:**950–958.
67. **Ross, T. M., and B. R. Cullen.** 1998. The ability of HIV type 1 to use CCR-3 as a coreceptor is controlled by envelope V1/V2 sequences acting in conjunction with a CCR-5 tropic V3 loop. Proc. Natl. Acad. Sci. USA **95:**7682–7686.
68. **Sattentau, Q. J.** 1998. HIV gp120: double lock strategy foils host defences. Structure **6:**945–949.
69. **Sattentau, Q. J., and J. P. Moore.** 1995. Human immunodeficiency virus type 1 neutralization is determined by epitope exposure on the gp120 oligomer. J. Exp. Med. **182:**185–196.
70. **Scarlatti, G., E. Trersoldi, A. Bjorndal, R. Fredriksson, C. Colognesi, H. K. Deng, M. S. Malnati, A. Plebani, A. G. Siccardi, D. R. Littman, E. M. Fenyo, and P. Lusso.** 1997. In vivo evolution of HIV-1 coreceptor usage and sensitivity to chemokine-mediated suppression. Nat. Med. **3:**1259–1265.
71. **Secchiero, P., D. Sun, A. L. De Vico, R. W. Crowley, M. S. Reitz, Jr., G. Zauli, P. Lusso, and R. C. Gallo.** 1997. Role of the extracellular domain of human herpesvirus 7 glycoprotein B in virus binding to cell surface heparan sulfate proteoglycans. J. Virol. **71:**4571–4580.
72. **Smyth, R. J., Y. Yi, A. Singh, and R. G. Collman.** 1998. Determinants of entry cofactor utilization and tropism in a dualtropic human immunodeficiency virus type 1 primary isolate. J. Virol. **72:**4478–4484.
73. **Speck, R. F., K. Wehrly, E. J. Platt, R. E. Atchison, I. F. Charo, D. Kabat, B. Chesebro, and M. A. Goldsmith.** 1997. Selective employment of chemokine receptors as human immunodeficiency virus type 1 coreceptors determined by individual amino acids within the envelope V3 loop. J. Virol. **71:**7136–7139.
74. **Stafford, M. K., D. Cain, I. Rosenstein, E. A. Fontaine, M. McClure, A. M. Flanagan, J. R. Smith, D. Taylor-Robinson, J. Weber, and V. S. Kitchen.** 1997. A placebo-controlled double blind prospective study in healthy female volunteers of dextrin sulfate gel: a novel potential intravaginal virucide. J.

Acquir. Immune Defic. Syndr. **14:**213–218.
75. **Sullivan, N., Y. Sun, Q. Sattentau, M. Thali, D. Wu, G. Denisova, J. Gershoni, J. Robinson, J. Moore, and J. Sodroski.** 1998. CD4-induced conformational changes in the human immunodeficiency virus type 1 gp120 glycoprotein: consequences for virus entry and neutralization. J. Virol. **72:** 4694–4703.
76. **Summerford, C., and R. J. Samulski.** 1998. Membrane-associated heparan sulfate proteoglycan is a receptor for adeno-associated virus type 2 virions. J. Virol. **72:**1438–1445.
77. **Thali, M., J. P. Moore, C. Furman, M. Charles, D. D. Ho, J. Robinson, and J. Sodroski.** 1993. Characterization of conserved human immunodeficiency virus type 1 gp120 neutralization epitopes exposed upon gp120-CD4 binding. J. Virol. **67:**3978–3988.
78. **Trkola, A., T. Dragic, J. Arthos, J. M. Binley, W. C. Olson, G. P. Allaway, C. Cheng-Mayer, J. Robinson, P. J. Maddon, and J. P. Moore.** 1996. CD4-dependent, antibody sensitive interactions between HIV-1 and its co-receptor CCR-5. Nature **384:**184–187.
79. **Trkola, A., A. B. Pomales, H. Yuan, B. Korber, P. J. Maddon, G. P. Allaway, H. Katinger, C. F. Barbas III, D. R. Burton, D. D. Ho, and J. P. Moore.** 1995. Cross-clade neutralization of primary isolates of human immunodeficiency virus type 1 by human monoclonal antibodies and tetrameric CD4-IgG. J. Virol. **69:**6609–6617.
80. **Trkola, A., M. Purtscher, T. Muster, C. Ballaun, A. Buchacher, N. Sullivan, K. Srinivasan, J. Sodroski, J. P. Moore, and H. Katinger.** 1996. Human monoclonal antibody 2G12 defines a distinctive neutralization epitope on the gp120 glycoprotein of human immunodeficiency virus type 1. J. Virol. **70:** 1100–1108.
81. **Tufaro, F.** 1997. Virus entry: two receptors are better than one. Trends Microbiol. **5:**257–260.
82. **Ueno, R., and S. Kuno.** 1997. Dextran sulfate, a potent anti-HIV agent in vitro having synergism with zidovudine. Lancet **i:**1379.
83. **Ugolini, S., I. Mondor, and Q. J. Sattentau.** 1998. HIV-1 attachment: a second look. Trends Microbiol. **7:**144–149.
84. **Ugolini, S., M. Moulard, I. Mondor, N. Barois, D. Demandolx, J. Hoxie, A. Brelot, M. Alizon, J. Davoust, and Q. J. Sattentau.** 1997. HIV-1 gp120 binding to $CD4^+$ cells induces an interaction between CD4, gp120 and the chemokine receptor CXCR4. J. Immunol. **159:**3000–3008.
85. **Verrier, F., A. M. Borman, D. Brand, and M. Girard.** 1999. Role of the HIV type 1 glycoprotein 120 V3 loop in determining coreceptor usage. AIDS Res. Hum. Retrovir. **15:**731–743.
86. **Warrier, S. V., A. Pinter, W. J. Honnen, M. Girard, E. Muchmore, and S. A. Tilley.** 1994. A novel, glycan-dependent epitope in the V2 domain of human immunodeficiency virus type 1 gp120 is recognized by a highly potent, neutralizing chimpanzee monoclonal antibody. J. Virol. **68:**4636–4642.
87. **Wu, L., N. P. Gerard, R. Wyatt, H. Choe, C. Parolin, N. Ruffing, A. Borsetti, A. A. Cardoso, E. Desjardin, W. Newman, C. Gerard, and J. Sodroski.** 1996. CD4-induced interaction of primary HIV-1 gp120 glycoproteins with the chemokine receptor CCR-5. Nature **384:**179–183.
88. **Wyatt, R., P. Kwong, E. Desjardins, R. W. Sweet, J. Robinson, W. A. Hendrickson, and J. G. Sodroski.** 1998. The antigenic structure of the HIV gp120 envelope glycoprotein. Nature **393:**705–711.
89. **Wyatt, R., J. Moore, M. Accola, E. Desjardin, J. Robinson, and J. Sodroski.** 1995. Involvement of the V1/V2 variable loop structure in the exposure of human immunodeficiency virus type 1 gp120 epitopes induced by receptor binding. J. Virol. **69:**5723–5733.
90. **Wyatt, R., and J. Sodroski.** 1998. The HIV-1 envelope glycoproteins: fusogens, antigens and immunogens. Science **280:**1884–1888.
91. **Wyatt, R., N. Sullivan, M. Thali, H. Repke, D. Ho, J. Robinson, M. Posner, and J. Sodroski.** 1993. Functional and immunologic characterization of human immunodeficiency virus type 1 envelope glycoproteins containing deletions of the major variable regions. J. Virol. **67:**4557–4565.
92. **Xiao, L., S. M. Owen, I. Goldman, A. A. Lal, J. J. deJong, J. Goudsmit, and R. B. Lal.** 1998. CCR5 coreceptor usage of non-syncytium-inducing primary HIV-1 is independent of phylogenetically distinct global HIV-1 isolates: delineation of consensus motif in the V3 domain that predicts CCR-5 usage. Virology **240:**83–92.